

Article

CO₂ Compression and Dehydration for Transport and Geological Storage

Paweł Bielka¹, Szymon Kuczyński^{2,*}  and Stanisław Nagy² ¹ Independent Researcher, 47-330 Zdzeszowice, Poland² Gas Engineering Department, Drilling, Oil and Gas Faculty, AGH University of Science and Technology, Mickiewicza 30 Av., 30-059 Kraków, Poland* Correspondence: szymon.kuczynski@agh.edu.pl

Abstract: Observation of the greenhouse effect prompts the consideration of every possibility of reducing anthropogenic carbon dioxide emissions. One of the key methods that has been the subject of much research is Carbon Dioxide Capture and Storage. The purpose of this study was to investigate the main technologies of CO₂ capture, separation, and dehydration as well as methods of its transport and methodology of selecting a suitable geological storage site. An installation of dehydration and compression of carbon dioxide captured after the post-combustion was designed at a temperature of 35 °C, a pressure of 1.51 bar, and a mass flow rate of 2.449 million tons/year, assuming that the geological storage site is located at 30 km from the capture place. For the dehydration process, a multistage compression and cooling system were applied, combined with a triethylene glycol (TEG) dehydration unit. The mass flow rate of TEG was selected as 0.5 kg/s. H₂O out of the TEG unit was 26.6 ppm. The amount of energy required to compress the gas was minimized by adopting a maximum post-compression gas temperature of 95 °C for each cycle, thereby reducing plant operating costs. The total power demand was 7047 kW, 15,990 kW, and 24,471 kW, and the total received heat input was 13,880.76 kW, 31,620.07 kW, and 47,035.66 kW for 25%, 60%, and 100% plant load, respectively. The use of more compressors reduces the gas temperature downstream through successive compression stages. It also decreases the total amount of energy required to power the entire plant and the amount of heat that must be collected during the gas stream cooling process. The integration of CO₂ compression and cooling system to recover heat and increase the efficiency of power units should be considered.

Keywords: CO₂ compression and dehydration; process simulation; TEG (triethylene glycol); CCS; carbon capture and storage



Citation: Bielka, P.; Kuczyński, S.; Nagy, S. CO₂ Compression and Dehydration for Transport and Geological Storage. *Energies* **2023**, *16*, 1804. <https://doi.org/10.3390/en16041804>

Academic Editors: Francesco Calise, Qiuwang Wang, Neven Duić, Poul Alberg Østergaard and Maria da Graça Carvalho

Received: 14 January 2023

Revised: 7 February 2023

Accepted: 8 February 2023

Published: 11 February 2023



Copyright: © 2023 by the authors. Licensee MDPI, Basel, Switzerland. This article is an open access article distributed under the terms and conditions of the Creative Commons Attribution (CC BY) license (<https://creativecommons.org/licenses/by/4.0/>).

1. Introduction

In recent years, progressive climate changes have been observed, causing undesirable atmospheric phenomena and negatively affecting the environment and living conditions on earth. Continuous development of economies and industrialization causes an increase in temperature, which has accelerated sharply in recent years.

Carbon dioxide is a greenhouse gas that has received special attention [1–3]. The highest CO₂ emissions occur for lignite and hard coal combustion. Greenhouse gas concentration increases in the atmosphere (other than water vapor), causing an increase in temperature, thus an increase in evaporation and an increase in the water vapor content in the atmosphere [4]. Progressive greenhouse effect forces consideration of every opportunity to reduce greenhouse gas emissions into the atmosphere.

In order to reduce CO₂ emissions to the atmosphere, CCS technology (Carbon Dioxide Capture and Storage) is applied by CO₂ capture, transport, and storage in geological formations [5,6]. CCS has recently attracted special attention. According to the European Green Deal, Europe intends to become the first climate-neutral continent by 2050. CCS

will allow the decarbonization of heavy industry, contributes to the initiation of a clean hydrogen economy, and will contribute to achieving zero net emissions [7].

Carbon dioxide captured from the flue gas at the point of emission has significant water content and needs to be dehydrated. Water content above the permissible values in the transported medium can cause the production of carbonic acid, which can block the flow [2]. The gas dehydration process avoids the formation of hydrates under the influence of high pressure and prevents corrosion of the installation. Dehydrated CO₂ needs to be pressurized to a desired pressure to be transported (i.e., by pipeline, gas carriers, rail, or trucks) to the storage site (injection installation). Each element of the CCS chain needs to be properly designed.

The projects completed so far and ongoing research related to CCS are characterized by various CO₂ dehydration technologies and installation configurations. Sholes consider the use of water-resistant composite membranes for CO₂ separation from methane [8]. Kemper, in his study, compared technologies of adsorption on molecular sieves and CO₂ dehydration with TEG [9]. Currently, the most common method for CO₂ dehydration is absorption with chemical solvents (using chemical bonds) or physical absorption, which uses the intermolecular Van der Waals forces [10]. The most commonly used physical solvents are: (i) Selexol™ technology based on glycol and (ii) Rectisol® based on methanol [11]. Chemical absorption (using amines) was used, i.e., in the post-combustion technology in two facilities—Boundary Dam (Canada) and Petra Nova (USA) [12]. For the Kingsnorth Carbon Capture & Storage Demonstration Project, molecular sieves technology was selected for CO₂ dehydration, although it is more expensive than the alternative TEG technology [13].

CO₂ dehydration is a relatively small part of the entire carbon capture and storage technology chain but plays a very important role in maintaining system integrity.

In case of high CO₂ emission allowances costs on the market, power plants and combined heat and power plants equipped with CCS installations using various gas dehydration technologies may become competitive.

In this study, the scenario of CO₂ dehydration and compression is considered. CO₂ captured from the emission source was directed to a multi-stage compression and cooling installation as well as dehydration of the captured CO₂ and its final compression for transport in a liquid state was designed. A combination of (i) multi-stage compression and cooling and (ii) a triethylene glycol (TEG) dehydration unit were designed for captured CO₂ dehydration. The influence of the number of compression stages on the efficiency of the installation as well as the demand for power and heat flux received in intercoolers was investigated.

2. Methodology

The methodology of the work assumes the discussion of individual components of the Carbon Capture and Storage (CCS) chain, as well as the selection of CO₂ capture technology which depends on the selected scenario. The methods of carbon dioxide separation were compared, and the appropriate method of CO₂ separation and compression was selected. CO₂ transport to the storage site was analyzed. Installation was designed, and simulations were performed with BRE Promax.

2.1. CO₂ Capture Technology

Carbon dioxide capture methods can be classified into:

- Post-combustion capture from flue gas in air-supplied fuels;
- Pre-combustion capture in gas obtained from the coal gasification process;
- Capture from the flue gas after combustion of fuel in boilers supplied with a mixture of oxygen and carbon dioxide (oxy-combustion);
- Methane steam-reforming process combined with carbon dioxide sequestration methods.

As CO₂ emissions are highest when burning lignite and hard coal, the plant was designed for post-combustion technology (Figure 1). The post-combustion carbon dioxide

capture involves separating CO₂ from other products that make up the flue gas (including, but not limited to, SO₂, NO_x, SO₂, and N₂) [4].

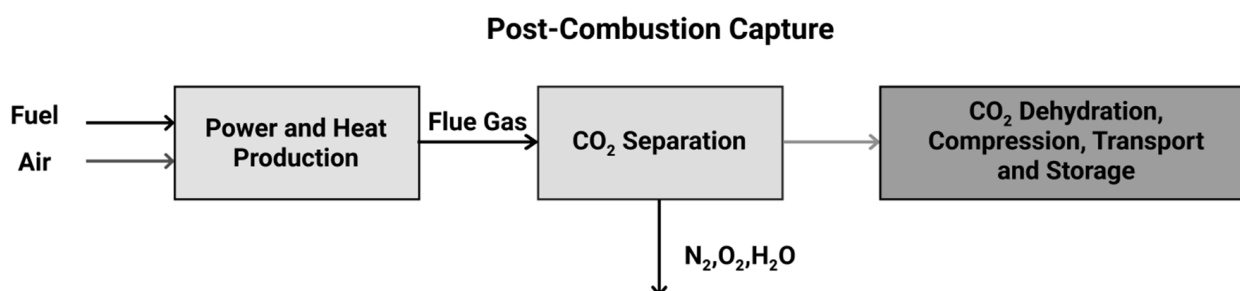


Figure 1. An overall diagram of the CCS technology for the application of the post-combustion process system.

2.2. Selection of the Carbon Dioxide Separation Method

The type of emission source and process system influences the selection of a suitable method for the separation of carbon dioxide from other combustion products (nitrogen, oxygen, nitrogen oxides, and sulfur). According to Czaplicki and Sobolewski, carbon dioxide separation can be performed based on physical and chemical absorption, adsorption, cryogenic, or membrane separation processes (Figure 2) [14].

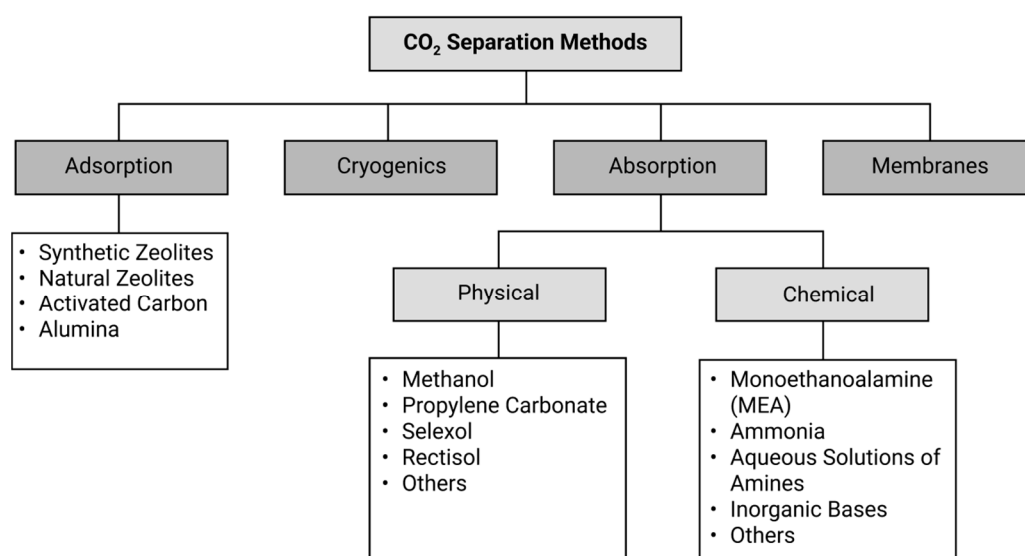


Figure 2. Carbon dioxide separation methods.

The suitable separation technology process is selected based on many factors, including the properties of flue gas—its pressure and temperature, CO₂ flow rate, or concentration [14–16].

2.3. Application of Multi-Stage Compression before TEG Dehydration

After capture, the gas must be further purified for further transport, as the contents of various components (water, sulfur and nitrogen oxides, oxygen, nitrogen, hydrogen sulfide) directly affect its chemical and physical parameters and process characteristics [14,17]. The H₂O content in the gas stream must be low enough to prevent corrosion of downstream plant components. Hydrogen sulfide and nitrogen dioxide do not directly affect the plant's condition or process efficiency. However, their minimum concentrations have been set for safety reasons [18].

Concentrations of individual volatile gases (N₂, H₂, CO, CH₄, O₂, Ar) should not exceed 4% [18,19].

The water content in the gas is a function of pressure and temperature [20]. The higher the pressure, the lower the H₂O content in the gas at a constant temperature, and the lower the temperature, the lower the water content at constant pressure. The method considered for the dehydration of gas captured from the emission source is the use of multistage compression with cooling. If the gas is compressed and then cooled to a constant temperature between compression stages, water will condense and must be drained off downstream each compression stage. However, this method is insufficient to ensure a sufficiently low H₂O content in the gas since the compressed gas is still saturated with water at the temperature to which it was cooled [20]. The most common gas dehydration method in the gas industry is absorption using liquid glycols due to the low plant cost compared to other dehydration methods [21]. The most commonly used glycol for gas dehydration is triethylene glycol (TEG) because it is recoverable to 98% and has higher sorptive properties [22]. Its advantages are [16]:

- Low vaporization loss and viscosity;
- High regeneration efficiency;
- High thermal stability;
- High affinity to water and hydrocarbon;
- Extremely low solubility for salts.

The use of triethylene glycol will ensure the dehydration of CO₂ to the appropriate H₂O content. However, multistage compression with cooling applied before the gas is dehydrated will reduce the cost of the TEG plant [20]. According to Øi and Fazlagic [23], the water content for different absorption pressures indicates that the maximum dehydration efficiency using TEG is achieved at pressures between 30 bar and 50 bar. Therefore, it was assumed that the pressure of gas supplied to the dehydration system for the plant designed should be 45 bar (without taking into account the pressure drop in the cooler). The constant temperature to which the gas will be cooled after each compression stage is assumed to be 20 °C. The number of compression stages affects the gas temperature downstream each compression stage.

In order to minimize the amount of energy required to cool the gas; it was assumed that its temperature after each compression cycle might not be higher than the assumed value of 95 °C [24]. In order to simplify the calculations, it was assumed that the efficiency of compressors and coolers for the first stage is 84%, and for subsequent stages, it is successively reduced by 2% [25].

The efficiency of the pump injecting the recovered glycol into the absorber column was taken as 70%. Panowski and Zarzycki [26] found that from the point of view of the lowest power demand, for the variant with similar final pressure (after multistage compression), the most beneficial would be the use of a system consisting of 5 or 6 groups of compression and cooling stages. It was assumed that the plant would consist of 5 compression and cooling stages before the gas enters the TEG dehydration system and of a final compression and cooling stage to prepare the CO₂ for further transport in its liquid state.

2.4. TEG Dehydration System

After five compression stages, cooling, and removal of released water, the gas goes to the TEG gas dehydration system. The first element of the plant is the absorber column. The gas stream is supplied to its lower part, where it flows in an upward direction through successive trays. At the same time, glycol is pumped through the upper section of the column, which flows by gravity down the subsequent absorber trays and absorbs water from the gas due to its absorption properties. The dehydrated gas leaves the system through the top of the column, and the water-rich glycol is automatically evacuated through the lower section of the column and supplied to its regeneration system.

After leaving the absorption column, the dehydrated gas stream is supplied to the final compression stage, where it reaches a pressure of 100 bar and is cooled down to a temperature of 20 °C so that it will change into a liquid state for cost-efficient transport. The rich glycol is expelled at the bottom of the column, and when preheated, it is supplied

to the deaerator. The water in the glycol is evaporated, and the lean glycol flows into a storage tank, from where it is supplied to the glycol make-up unit. Stripping gas can be added to the reboiler or stripping column to improve the regeneration of TEG [23]. The TEG decomposition temperature should be in the range of 180–207 °C, so it was established that the gas in the reboiler would be heated to the temperature of 205 °C [27,28].

Depending on the expected mass flow rate of lean glycol re-injected into the absorber column, different values of H₂O gas purification can be obtained. Choosing the correct amount of glycol for replenishment allows for the reduction in the operating costs of the glycol regeneration system. Choosing an excessively low mass flow rate of lean glycol entering the absorber column can result in insufficient gas dehydration, but efforts should be made to reduce the amount of glycol for replenishment to reduce costs [29].

Too small a mass flow of lean glycol, which flows to the absorber column, may result in insufficient drying of the gas [20,25]. However, the amount of supplemented glycol should be limited to reduce costs because the higher the glycol flow rate is, the larger column diameter is required, which translates into higher investment costs [29].

2.5. Transport of CO₂ to a Geological Storage Site

The purified and compressed carbon dioxide must be delivered to the storage site by pipelines, road tankers, or carriers. The most efficient form of transport is the transfer of CO₂ via pipelines [30,31]. Transporting CO₂ via a pipeline is more cost-effective than transporting it by road tankers or carriers because it can provide a continuous supply chain from the capture plant to the injection site. More than 8000 km of pipelines are in the United States, which is 85% of Global pipelines transporting CO₂ [10]. Technically, CO₂ can be transported in gaseous, liquid, or supercritical phases. However, the minimum pipeline operating pressure should be selected to ensure that CO₂ is transported in the liquid or supercritical phase [30].

Transport of carbon dioxide in the gaseous phase is problematic because the maximum discharge pressure can reach 40 to 45 bar. Exceeding these pressure values causes CO₂ to condense, thus creating a two-phase flow, which can result in damage to pipeline fittings [32,33]. Transporting CO₂ in the gaseous phase is an inefficient and energy-intensive process due to the large pressure drops in the pipeline with low density of the gaseous phase [30–32].

A more efficient way to transfer CO₂ than transporting it in the gaseous phase is to transfer it in the supercritical state. The supercritical state is called the state of a substance in which the pressure and temperature conditions have exceeded the critical point of the substance, and the substance itself has viscosity and compressibility parameters characteristic of a gas while having the density of a liquid [30]. This allows much greater quantities of CO₂ to be transported and stored than possible in its gaseous form. The critical point of carbon dioxide ($T_c = 30.978$ °C, $p_c = 73.773$ bar), for which the density of CO₂ is equal to $\rho = 467.6$ kg/m³, allows its transfer at high pressures ranging from 80 bar to 150 bar [34].

CO₂ transport requires its compression to high pressure (74 bar should be taken as the absolute minimum, but usually it is 100 bar, which provides an appropriate safety margin related to pressure drop in the pipelines). After leaving the absorption column, dehydrated CO₂ in gaseous form can be directed to the final compression, where it reaches a pressure of 100 bar and is cooled down to 20 °C [10]. As a result, CO₂ becomes a liquid, which allows it to be transported economically.

The minimum pressure in the pipeline should be equal to or higher than 73.8 bar, which means that CO₂ will remain in a supercritical state. While there are slight variations in the pressure ranges in the literature, all pressures are above the critical value of 73.8 bar [35].

The transport of CO₂ in the supercritical state is not without its drawbacks. As the length of the pipeline increases, the carbon dioxide temperature decreases. If the temperature drops below the critical value, CO₂ will change into a liquid phase, and if pressure drops rapidly, it will change into a gaseous phase. The temperature must be therefore maintained in the pipeline—a highly energy-consuming process [30].

From the economic viewpoint, the transfer of carbon dioxide in the liquid state is the most advantageous form of transport [36–39]. Carbon dioxide in liquid form has a slightly higher density than in the supercritical state while maintaining low compressibility. Obtaining CO₂ in a liquid form requires that it be compressed and cooled to the proper pressure and temperature before being injected into a pipeline. Carbon dioxide should be thoroughly dried to a water content of less than 50 ppm_v, as exceeding this value affects corrosion activities on pipeline fittings and walls [40]. The composition of the treated and compressed gas stream should meet the recommended requirements for the content of individual gas components (Table 1).

Table 1. Recommended permissible concentrations of relevant components of the gas stream for further transport.

Gas Stream Component	Unit	Recommended Molar Concentration	Source
CO ₂	%	>95	[41,42]
H ₂ O	ppm _v	<50	[41–43]
H ₂ S	ppm _v	<(10–50)	[41,42]
O ₂	ppm _v	<10	[41,42]
N ₂	%	<4	[41,42]
H ₂	%	<4	[41,42]
Ar	%	<4	[41,42]
CO	ppm _v	<2000	[41,43]
Nitrogen oxides (NO _x)	ppm _v	<100	[44,45]
Sulfur oxides (SO _x)	ppm _v	<50	[44]
Hydrocarbons (HC)	%	<2	[41,45]

2.6. Selection of a Geological Carbon Dioxide Storage Site

Carbon dioxide can be injected into a natural geological formation located on land or under the ocean or seafloor. It was assumed that the depth below which CO₂ passes through the critical point to the supercritical phase is a depth of about 800 m [4,46–48]. Thus, this is the minimum depth of the roof of the layers intended for the geological storage of carbon dioxide.

The geological formation into which CO₂ is to be injected must be characterized by the presence of porous and permeable rocks that are covered by a layer of impermeable rocks [4,46]. This will allow it to accumulate in interstitial spaces and cracks. Thus CO₂ displaces and replaces substances such as water, oil, or gas. The Polish National Geological Institute (2020) [49] formulates the main criteria for potential CO₂ reservoirs:

- Appropriate values for permeability, porosity, and potential reservoir capacity;
- The presence of geological traps and impermeable cover rocks (e.g., clays, marls, salt rocks, and claystone) will prevent carbon dioxide from migrating to higher layers;
- Aquifers must not contain potable water that humans can use;
- The reservoir should be located more than 800 m below the ground surface due to providing conditions of high enough pressure and temperature to store carbon dioxide in the supercritical state.

About 99% of the global CO₂ storage capacity is saline aquifers, and the rest are depleted oil and gas reservoirs and coalbed methane [50].

2.7. Pipeline Transport

At the existing CCS facilities, the pipelines leading to the storage facility differ in length. For example, in Norway, a 153 km offshore pipeline operates at the Snøhvit CO₂ storage site [10].

In this study, the geologic storage site was assumed to be within 30 km of distance from the TEG dehydration unit. The pipeline has a length of 30 km and has been divided into four segments of 7500 m each.

According to Polish standards, the pipeline should be located away from densely populated areas and meet the technical conditions according to the Ordinance of the Minister of Economy of 26 April 2013, on technical conditions to be met by gas networks and their location [51]. Before being injected into the pipeline, CO₂ must also be tested for its impurity content and its properties.

The pipeline diameter should be selected to ensure effective carbon dioxide transmission while keeping investment and operating costs as low as possible since they increase as the diameter of the pipeline increases. The materials used for the pipeline should prevent corrosion, whereas fittings and seals should provide adequate strength for cold temperatures caused by CO₂ expansion in the pipeline [52,53]. The selection of materials requires an analysis of the conditions in which the pipeline will operate, including ambient conditions and the composition of the medium being transported. According to API 5L standards, steel grades X60, X65, and X70, among others, are used for CO₂ transport pipelines, and X80 steel [30,54] when large diameters are used at operating pressures of approximately 160 bar (Table 2). These steel grades are characterized by high tensile strength and also high yield strength.

Table 2. Comparison of chemical composition and selected parameters of selected steel grades according to API 5L.

Chemical Element	Steel Grade			
	API 5L X60	API 5L X65	API 5L X70	
C	0.16	0.16	0.17	
Si	0.45	0.45	0.45	
Mn	1.65	1.65	1.75	
P	0.02	0.02	0.02	
S	0.01	0.01	0.01	
V	0.08	0.09	0.1	
Nb	0.05	0.05	0.05	
Ti	0.04	0.06	0.06	
Yield point	bar	4136.9	4881.59	4826.33
Tensile strength	bar	5171.07	5308.96	5653.7
Elastic modulus		0.93	0.93	0.93
Static elongation	%	19	18	17

2.8. Simulation of the Operation of the Planned Plant in BR&E ProMax

BR&E ProMax software, developed by Bryan Research & Engineering Inc., was used to simulate the planned dehydration, compression, and further carbon dioxide plant transport. This software is used for the simulation of processes and is dedicated to specific chemical and petrochemical processes, among others:

- Dehydration processes with glycols and desulfurization with amine solutions;
- Refining processes;
- LPG recovery processes;
- Gas cooling and processing;
- Calculations and simulations for pipeline transportation and chemical and petrochemical processes.

3. Results and Discussion

A diagram of the planned five-stage captured gas compression and cooling plant designed in ProMax is shown in Figure 3, captured gas dehydration plant with TEG is shown in Figure 4, and the gas compression, cooling, and injection plant into the transmission pipeline are shown in Figure 5. The Peng-Robinson equation of the state model was used to perform the simulation [55].

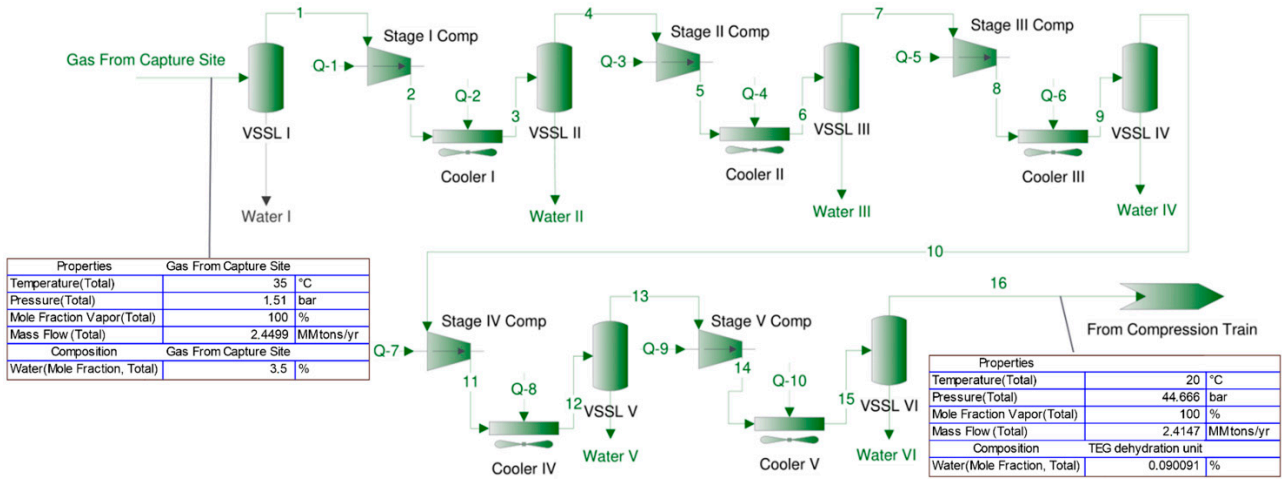


Figure 3. CO₂ compression train (first part of the plant).

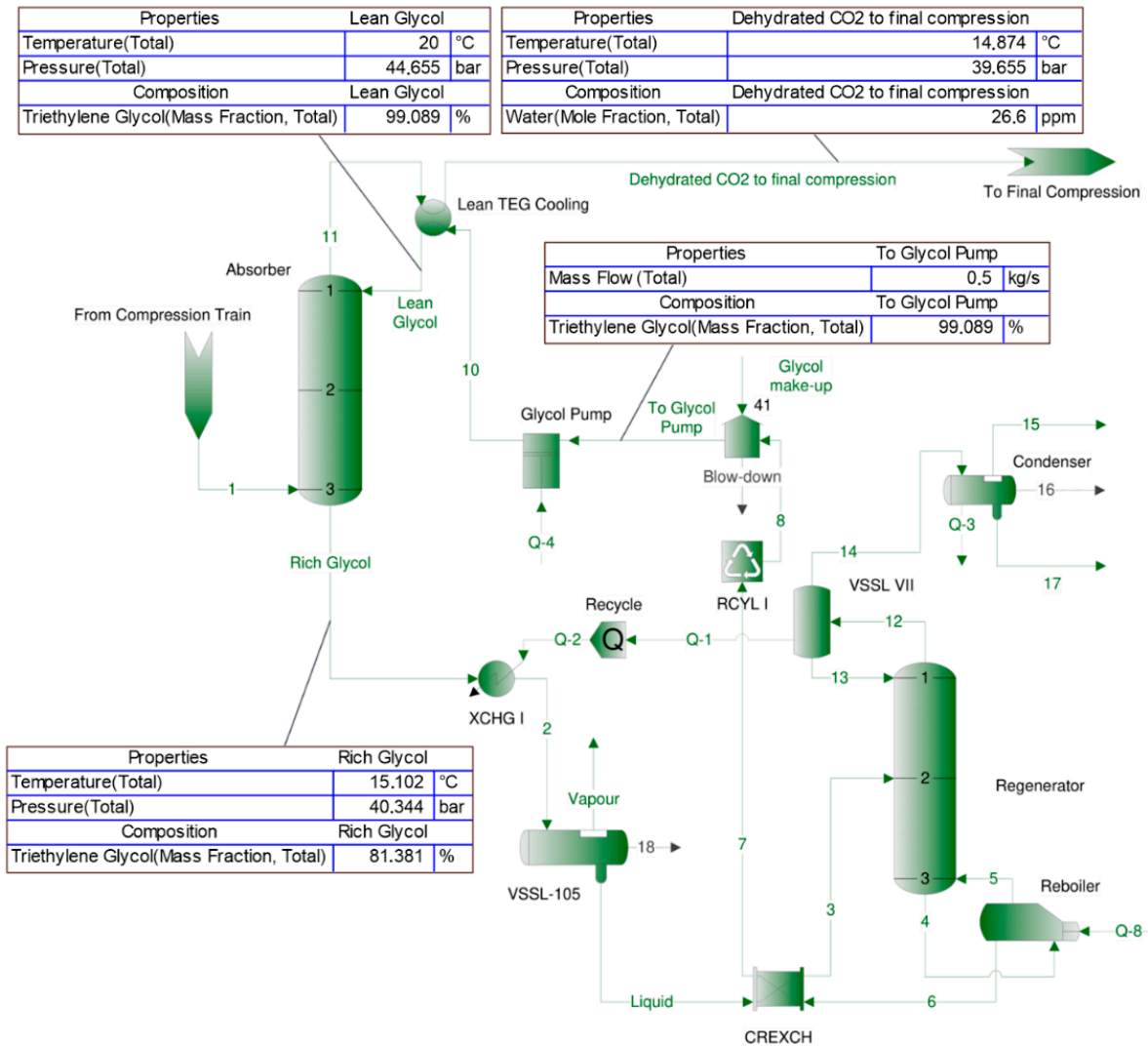


Figure 4. TEG dehydration plant (second part of the plant).

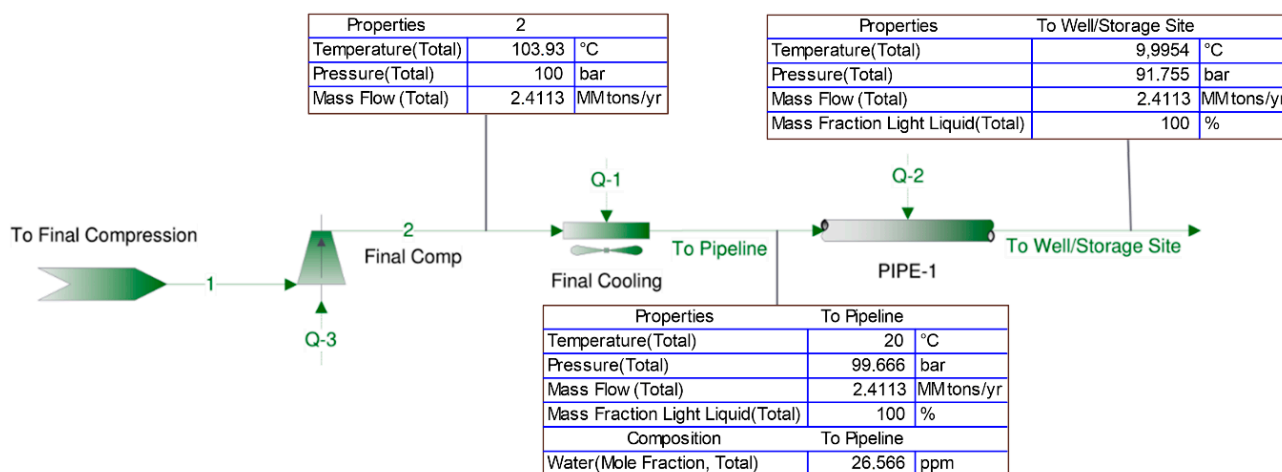


Figure 5. Final compression, cooling, and transport to the storage site.

3.1. Input Data

In order to simulate the process of treatment and compression of the gas for further transport and injection into the geological formation, it was assumed that the captured gas compression and treatment plant is located onshore at the emission source. The post-combustion captured gas stream at 35 °C, and 1.51 bar should be purified to the recommended molar concentrations of the individual components and compressed to the pressure at which it reaches a liquid state. The plant will be designed to prepare 2.449 million tons/year of carbon dioxide for transport and injection at 100% of its load. Transport of the liquid CO₂ to the geological storage site will take place via a 30 km long onshore pipeline. The contents of each component of the captured gas and its temperature and pressure conditions are shown in Table 3.

Table 3. Molar concentrations of individual components of the captured gas and inlet flow parameters are assumed for design purposes.

Captured Gas Component	Unit	Value
CO ₂	%mol	96.45
H ₂ O	%mol	3.5
N ₂	%mol	0.03
O ₂	%mol	0.02
Inlet gas stream parameters		
Temperature	°C	35
Pressure	bar _a	1.51
Mass flow rate	million tons/year	2.449

The captured gas stream with a mass flow rate of 2.449 million tons/year, a temperature of 35 °C, a pressure of 1.51 bar, and a molar concentration of the individual substances, as shown in Table 4, is initially directed to a separator, where the liquid phase of the input stream is separated from its gas phase. Water flows by gravity into the lower section of the separator, from where it is discharged. The gas leaves the separator through its upper section and is directed to the first compression and cooling cycle. After the gas stream is compressed and cooled to 20 °C, it enters the separator from which the water formed by the pressure increase at constant temperature is removed. The gas compression and cooling cycle are repeated five times. To reduce the operating costs of the compression system, the temperature at which the maximum compression pressure will be reached is set to 95 °C.

Table 4. Pressures and temperatures of the gas stream after each compression cycle.

Compression Stage	Max. Pressure for T < 95 °C	Assumed Pressure	Gas Temperature after Compression
	bar	bar	°C
Captured gas		1.51	35
1	3.017	3	94.483
2	6.850	6.8	94.316
3	15.523	15.2	94.812
4	33.260	33	94.209
5	71.110	45	49.543

3.2. Permissible Pressure Drops across Coolers

The value of permissible pressure drops across intercoolers was determined using Equation (1) while assuming that the value of permissible pressure drop cannot be greater than 0.334 bar [56].

$$\Delta p = \frac{(14.504 \cdot p_{CO_2/Stage})^{0.7}}{10 \cdot 14.504}, \text{ bar} \quad (1)$$

where:

$p_{CO_2/Stage}$ —the value of CO₂ pressure for the individual compression stage, bar.

Individual values of allowable pressure drop across the coolers were obtained for successive compression stages (Table 5).

Table 5. The values of obtained acceptable pressure drop across coolers.

Compression Stage	p_{CO_2} , bar	Δp , bar
1	3	0.097
2	6.8	0.172
3	15.2	0.301
4	33	0.518 > 0.334
5	45	0.644 > 0.334
6 (after final compression)	100	1.126 > 0.334

3.3. Selection of the Glycol Mass Flow Rate

For the designed plant, the mass flow rate of glycol entering the absorber column was chosen as 0.5 kg/s since it provides a proper level of CO₂ drying, equal to 26.6 ppm. The water content in CO₂ for the selected TEG mass flow rate meets the recommended requirements for CO₂ transport via transfer pipelines (Table 6).

Table 6. Changes in the dried gas composition depend on the expected mass flow of glycol after the regeneration process.

Glycol Mass Flow kg/s	CO ₂ %	H ₂ O ppm _v	N ₂ %	O ₂ %	TEG %
0.1	99.9384	97.5	0.03109	0.0207	5.60×10^{-6}
0.15	99.9419	62.2	0.03109	0.0207	6.30×10^{-6}
0.2	99.9435	46.1	0.3110	0.0207	6.77×10^{-6}
0.25	99.9444	37.8	0.03111	0.0207	6.99×10^{-6}
0.3	99.9448	33.2	0.03111	0.0207	7.12×10^{-6}
0.5	99.9454	26.6	0.03112	0.0207	7.40×10^{-6}

3.4. Pipeline Diameter

The selection of pipeline parameters, including its diameter, is an issue that requires consideration of several conditions, both technical and logistic [30]. The main factors

determining the pipeline diameter include the pressure at the beginning and the end of the pipeline, the temperature in the pipeline, the pipeline length, the flow rate of carbon dioxide transported, and the number of compressor stations installed along the pipeline [36].

The pipeline diameter should ensure the reception of liquid carbon dioxide. Therefore, it was assumed that the minimum pipeline operating pressure should be 80 bar for a CO₂ stream temperature of 20 °C. For a mass flow rate at 100% plant load equal to 2.449 million tons/year, a comparative simulation of the distances for which the pressure will reach the assumed minimum pipeline operating pressure was performed. For a pipeline diameter of 16 inches, the pipeline pressure will reach 80 bar for 251 km, which means that the use of the adopted diameter is reasonable (Figure 6a). For a 14-inch diameter pipeline of the same material, the pressure in the pipeline will reach 80 bar at 112 km (Figure 6b). For an assumed pipeline diameter of 12 inches (Figure 6c), the minimum operating pressure of the pipeline equal to 80 bar will be reached at 68 km. Selecting a smaller pipeline diameter (10 inches) does not provide proper pressure for the specified 30 km pipeline segment to transport CO₂ to the storage site (Figure 6d). The pipeline pressure reaches 80 bar over a distance less than the planned pipeline length (26 km). Based on the above considerations, a pipeline diameter of 12 inches was selected for further research.

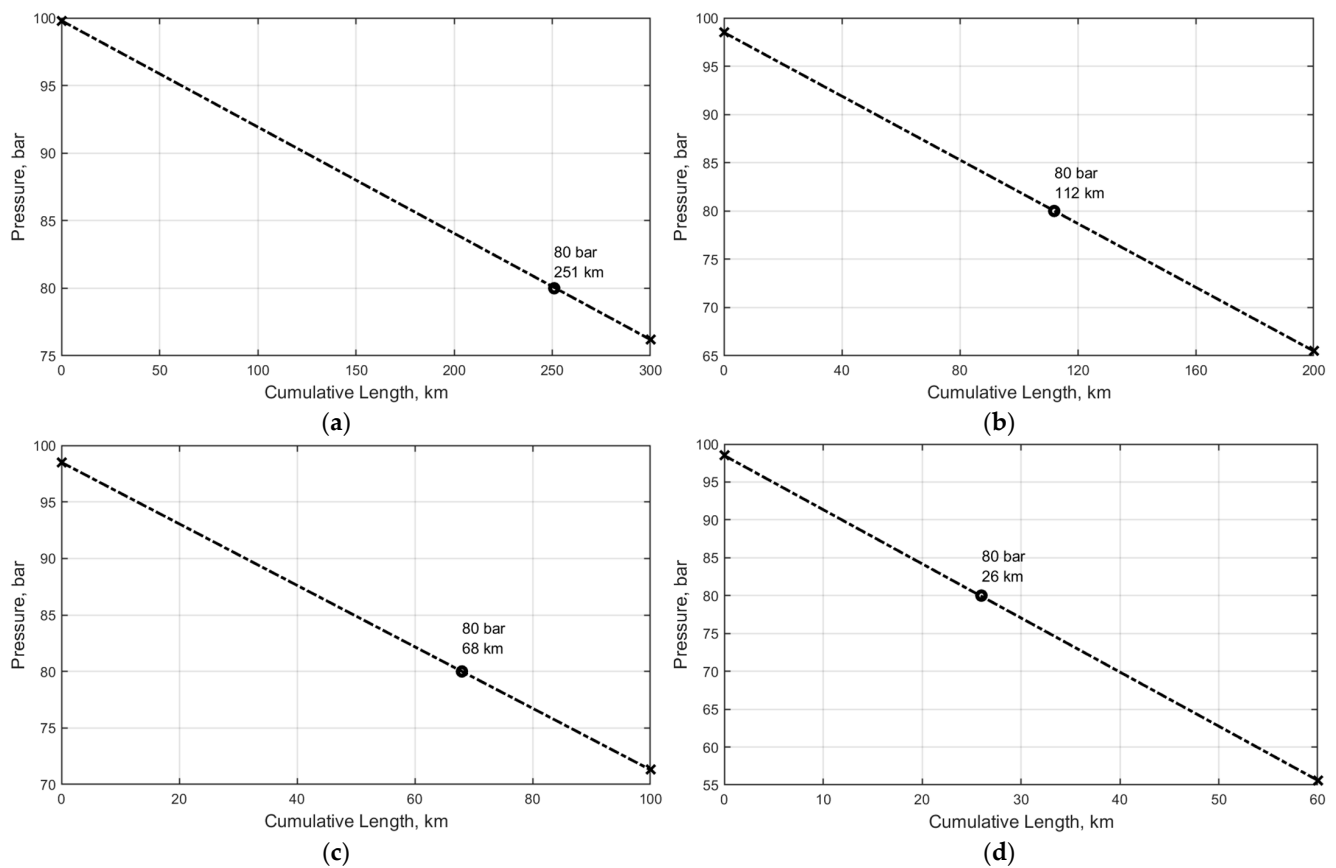


Figure 6. The distance over which the minimum operating pressure for a variant pipeline diameter will reach the 80 bar limit for X70 steel. (a) 16-inch diameter pipeline; (b) 14-inch diameter pipeline; (c) 12-inch diameter pipeline; (d) 10-inch diameter pipeline.

A similar method to determine the pipeline diameter is to assume the pressure at the pipeline outlet and to select, based on the pipeline specifications, the maximum amount of CO₂ that can be transported while maintaining its liquid state. Knowing the parameters beyond which the two-phase flow will occur and the possible formation of hydrates (carbonic acid), as well as knowing the rate at which CO₂ will be injected into the pipeline, it is possible to control the pipeline diameter in order to analyze the distance of the pipeline

over which the CO₂ pressure drop to the assumed value of 80 bar will be achieved. The use of the analysis in ProMax software allows for the selection of a diameter that will ensure the transport of carbon dioxide while maintaining proper parameters over the considered distance of 30 km. However, the results obtained will be similar to the results obtained by means of manual determination of the diameter.

The length of the pipeline system assumed above has been simplified and can be understood as an equivalent length due to the difficulty of determining local pressure losses at the conceptual stage of research. The proper distance from the storage site is less than the assumed length of the pipeline, and this value is intended to provide an overview of the pressure drop distribution.

3.5. Linear Pressure Drop

When considering pipeline transport of carbon dioxide, the linear pressure drop in the pipeline must be considered, and it must be verified that the pressure at the pipeline end is not less than the assumed minimum pressure (80 bar) to allow carbon dioxide to be received in its liquid state. For this purpose, the Darcy Weisbach Equation (2) was used [22]:

$$\Delta p = \lambda \cdot \frac{L}{D} \cdot \frac{\rho \cdot u^2}{2 \cdot 10}, \text{ bar} \quad (2)$$

where:

λ —coefficient of linear pressure losses;

L —pipeline segment length, m;

D —pipeline diameter, m;

ρ —fluid density, kg/m³;

u —fluid velocity, m/s.

In order to determine the pressure, drop, the value of the resistance coefficient λ must be determined from Equation (3). For this purpose, the value of the roughness coefficient of the pipe's inner surface was assumed to be 0.00004 [57].

$$\frac{1}{\lambda} = -2 \log \cdot \left(\frac{\frac{\epsilon}{D}}{3.7} + \frac{2.51}{Re \cdot \sqrt{\lambda}} \right) \quad (3)$$

where:

$\frac{\epsilon}{D}$ —pipe inner surface roughness coefficient;

Re —Reynolds number.

In order to calculate the linear pressure loss coefficient, the pattern of the fluid flow in the transmission pipeline must be determined. The basic criterion for determining the pattern of fluid flow is the Reynolds number, which can be defined by Equation (4) [22]:

$$Re = \frac{u \cdot D \cdot \rho}{\mu}, \quad (4)$$

where:

μ —dynamic fluid viscosity, Pa·s.

The dynamic viscosity value for the fluid inlet flow determined using the ProMax simulation software is 8.21375×10^{-5} Pa·s. The fluid velocity is equal to (5):

$$u = \frac{\dot{m}}{\pi \cdot \frac{D^2}{4} \cdot \rho} \quad (5)$$

where:

\dot{m} —fluid mass flow, kg/s.

By using the above formulas, the value of linear pressure drop was determined for four equal pipeline segments, each 7500 m long. The obtained values of fluid velocity parameters, Reynolds number, flow resistance coefficient, and linear pressure drop values

are summarized in Table 7. The results were compared with the linear pressure drop values obtained from the ProMax simulation.

Table 7. Linear pressure drops for successive pipeline segments.

Parameter	Symbol	Value	Unit
Fluid velocity	u	1.452	m/s
Reynolds number	Re	4,528,426	
Flow resistance coefficient	λ	0.011	
Linear pressure drop for 1 pipe segment	Δp	2.18	bar
Total linear pressure drop	$4 \cdot \Delta p$	8.72	bar

Linear pressure drop				
Pipeline length	Darcy-Weisbach equation		Simulation results	
	Δp	Pressure in pipeline	Δp	Pressure in pipeline
m	bar	bar	bar	bar
7500	2.18	97.82	2.13958	97.86042
15,000	4.36	95.64	4.28206	95.71794
22,500	6.54	93.46	6.42743	93.57257
30,000	8.72	91.28	8.57571	91.42429

The obtained values of linear pressure drop differ slightly, which may be due to the assumed approximations and a different calculation model in ProMax software. The final calculated pressures in the pipeline do not exceed the assumed minimum operating pressure of 80 bar.

3.6. Energy Required to Power the Plant for Its Different Loads

The amount of energy required to power the planned plant was analyzed for 25%, 60%, and 100% load, respectively. The parameters characterizing the input captured gas flow depend on the selected plant load level, and the obtained values of power demand and heat flux collected in the coolers of the plant are shown in Table 8. The total power demand is 7047.57 kW, 15,990.10 kW, and 24,471.75 kW, respectively, and the total heat flux collected is 13,880.76 kW, 31,620.07 kW, and 47,035.66 kW for 25%, 60%, and 100% plant load, respectively (Table 9). A similar analysis was planned for the Kingsnorth Carbon Dioxide Capture and Storage Demonstration Project using MEA. However, the results were not presented [13].

Table 8. Inlet gas flow parameters vs. plant load.

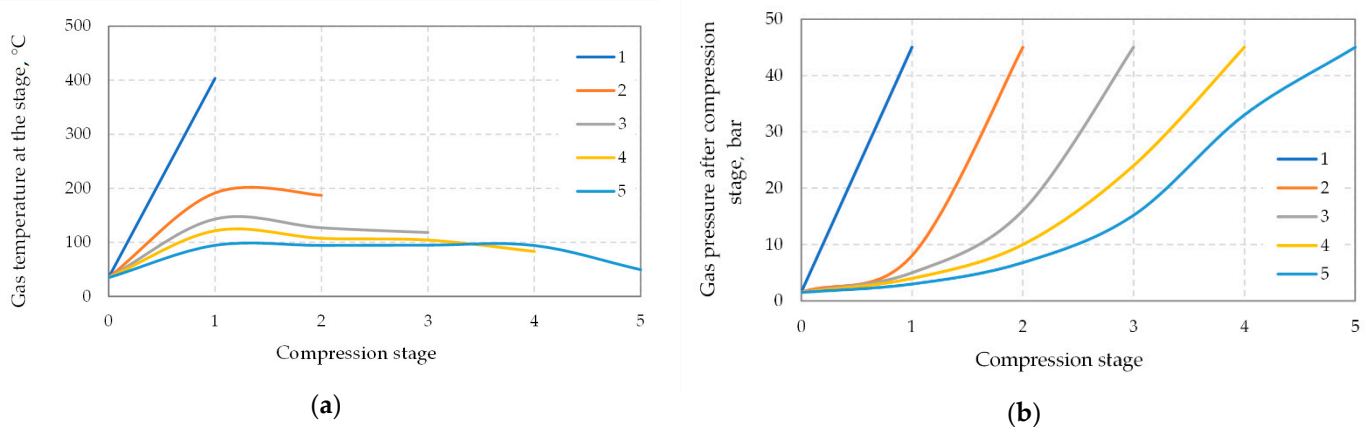
Parameter	Unit	25% Load	60% Load	100% Load
Temperature	°C	35	35	35
Pressure	bar _a	1.51	1.51	1.51
Mass flow rate	million tons/year	0.719	1.636	2.449
Molar flow rate	kmol/h	1906	4334	6490

For assumed parameters, simulations were performed to determine the power demand of the designed gas compression and cooling train (100% load) to reach 45 bar and 20 °C—desired conditions under which gas should be supplied to the TEG dehydration unit. Calculations were performed for five scenarios starting from single-stage compression to five-stage compression.

Table 9. Balance of energy required to power the compression and dehydration plant and energy of the heat flux collected.

Installation Stage	Installation Element	25% Load Power Demand, kW (Compressors) Collected Heat Flux Power, kW (Coolers)	60% Load	100% Load
Pre-compression and cooling before delivery to the TEG plant	Compressor I	1203.33	2736.22	4097.39
	Cooler I	2160.97	4913.77	7358.19
	Compressor II	1434.47	3261.8	4884.43
	Cooler II	1620.96	3865.85	5519.41
	Compressor III	1393.7	3169.09	4745.59
	Cooler III	1633.71	3714.85	5562.84
	Compressor IV	1289.71	2932.63	4931.5
	Cooler IV	1796.56	4085.15	6117.35
	Compressor V	434.199	987.313	1478.46
	Cooler V	867.354	1972.25	2953.37
	Total power demand	5755.409	13,087.053	20,137.37
	Total collected heat flux power	8079.554	18,551.87	27,511.16
Preparation of dehydrated CO ₂ for pipeline transport	Pump VI	1292.16	2903.05	4334.38
	Cooler VI	5801.2	13,068.2	19,524.5
	Total power demand	1292.16	2903.05	4334.38
	Total collected heat flux power	5801.2	13,068.2	19,524.5
Total power demand		7047.569	15,990.103	24,471.75
Total collected heat flux power		13,880.754	31,620.07	47,035.66

Figure 7 shows that when single- or two-stage compression is used, the pressure and temperature values obtained far exceed the capabilities of commercially available compressors. The use of more compression stages affects the temperature downstream of the compression stage. For the use of 3, 4, or 5 compression stages, the temperature values are practically the same, although an increase in the number of compression stages with intercooling results in a decrease in the total amount of energy required to power the entire plant. At the same time, it can be observed that as more compression stages are used, the amount of heat that can be collected during the gas stream cooling process decreases, which limits the possibility of using it in the thermal cycle of the power unit (Figure 8).

**Figure 7.** Pressure (a) and temperature (b) distributions for successive groups of compression stages.

The application of multistage compression with interstage cooling results in a decrease in the efficiency of the power unit by approximately 6.5% in the optimistic variant, which translates into a decrease in the net efficiency of electricity generation at the level of 39% (currently constructed power units show a net efficiency of more than 45%) [26]. Therefore, it is reasonable to consider the integration of CO₂ compression and cooling systems to recover heat and increase the efficiency of power units.

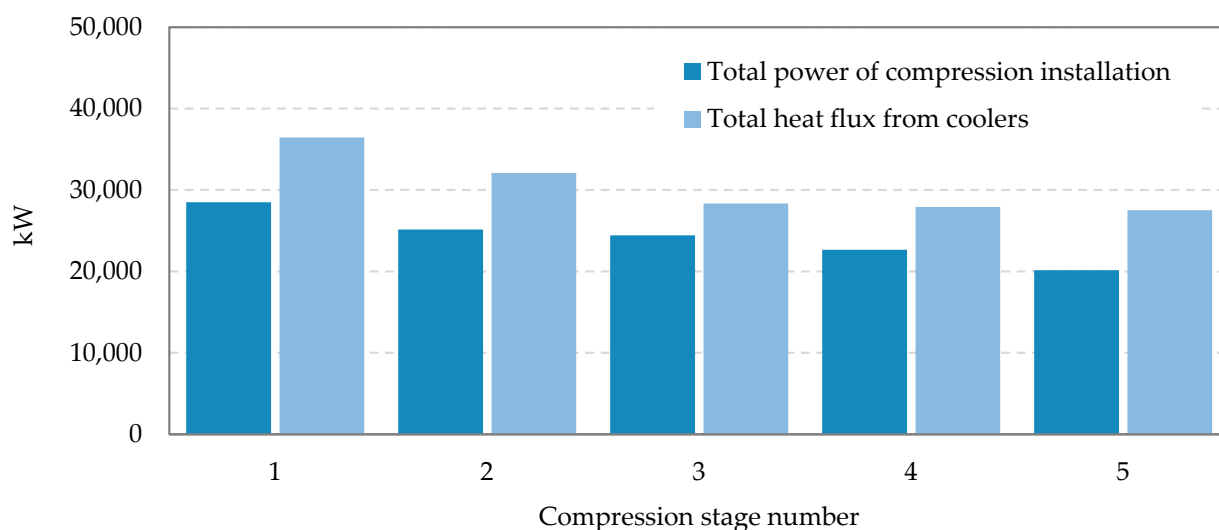


Figure 8. Power demand and heat flux collected in coolers versus the number of compression stages.

4. Conclusions

Based on the assumed input data for the considered scenario, the following design findings were obtained:

- The temperature at which the maximum compression pressure is reached will not exceed 95 °C;
- The mass flow rate of glycol supplied to the absorber column was chosen to be 0.5 kg/s as it provides an adequate level of CO₂ dehydration, amounting to 26.6 ppm;
- The pipeline to receive liquid carbon dioxide from the TEG plant and inject it into the geological storage site has a determined diameter of 12 inches;
- At a distance of 30 km from the geological storage site, the value of the linear pressure drop was 8.72 bar (obtained using the Darcy Weisbach equation) or 8.57 bar (using ProMax software simulation);
- The total power demand is 7047.57 kW, 15,990.10 kW, and 24,471.75 kW, and the total received heat input is 13,880.76 kW, 31,620.07 kW, and 47,035.66 kW for 25%, 60%, and 100% plant load, respectively.

A multi-stage compression system and a TEG dehydration system were used as a method to dehydrate carbon dioxide to the required values. The number of compression and intercooling cycles was determined to be 5, whereas the placement of this system upstream of the TEG dehydration system reduced its operating costs. By adopting a maximum post-compression temperature for each cycle, the energy required to compress the gas was minimized, thereby reducing plant operating costs. With the glycol mass flow rate selected as 0.5 kg/s, H₂O content at the outlet of the TEG system was 26.6 ppm, N₂ approximately 0.0311%, and oxygen 0.0207% at a TEG concentration of $7.4 \times 10^{-6}\%$.

The choice of state of aggregation in which CO₂ is to be transported depends on the distance from its geological storage site and the injection pressure. Regarding the thermodynamic aspect, the transport of carbon dioxide in the supercritical state is the most advantageous as it preserves the density of the liquid with the compressibility and viscosity of the gas; however, due to the process and technological aspects, the transport of CO₂ in the liquid phase was chosen while meeting the conditions of supercritical pressure.

Using more compressors and intercooling reduces the gas temperature downstream through successive compression stages. Furthermore, as the number of compression stages increases, the total energy required to power the entire plant and the amount of heat that must be collected during the gas stream cooling process decreases.

Author Contributions: Conceptualization, S.N., S.K., and P.B.; methodology, S.K. and P.B.; validation, S.K.; formal analysis, S.K. and P.B.; investigation, S.K. and P.B.; resources, S.K. and P.B.; data curation, S.K. and P.B.; writing—original draft preparation, S.K. and P.B.; writing—review and editing, S.K. and P.B.; visualization, S.K. and P.B.; supervision, S.K. and S.N.; funding acquisition, S.N. All authors have read and agreed to the published version of the manuscript.

Funding: This research was funded by EEA and Norway Grants, operated by The National Center for Research and Development, grant number NOR/POLNORCCS/AGaStor/0008/2019-00.

Data Availability Statement: Publicly available datasets were analyzed in this study.

Acknowledgments: Special thanks to Joanna Nizioł.

Conflicts of Interest: The authors declare no conflict of interest.

References

1. Udara Willhelm Abeydeera, L.H.; Wadu Mesthrige, J.; Samarasinghalage, T.I. Global Research on Carbon Emissions: A Scientometric Review. *Sustainability* **2019**, *11*, 3972. [CrossRef]
2. Balat, M.; Balat, H.; Acici, N. Environmental Issues Relating to Greenhouse Carbon Dioxide Emissions in the World. *Energy Explor. Exploit.* **2003**, *21*, 457–473. [CrossRef]
3. World Resources Institute. Available online: <https://www.wri.org/our-work/project/cait-climate-data-explorer> (accessed on 2 January 2023).
4. Dubiński, J.; Wachowicz, J.; Koterak, A. Underground storage of carbon dioxide—The possibilities for using CCS technology in Polish conditions. *Górnictwo i Geol.* **2010**, *5*, 5–19.
5. Li, Q.; Wang, F.; Forson, K.; Zhang, J.; Zhang, C.; Chen, J.; Wang, Y. Affecting analysis of the rheological characteristic and reservoir damage of CO₂ fracturing fluid in low permeability shale reservoir. *Environ. Sci. Pollut. Res.* **2022**, *29*, 37815–37826. [CrossRef]
6. Postma, T.J.; Bandilla, K.W.; Celia, M.A. Implications of CO₂ mass transport dynamics for large-scale CCS in basalt formations. *Int. J. Greenh. Gas Control* **2022**, *121*, 103779. [CrossRef]
7. van Renssen, S. The hydrogen solution? *Nat. Clim. Change* **2020**, *10*, 799–801. [CrossRef]
8. Sholes, C.A. Water Resistant Composite Membranes for Carbon Dioxide Separation from Methane. *Appl. Sci.* **2018**, *8*, 829. [CrossRef]
9. Kemper, J.; Sutherland, L.; Watt, J.; Santos, S. Evaluation and analysis of the performance of dehydration units for CO₂ capture. *Energy Procedia* **2014**, *63*, 7568–7584. [CrossRef]
10. Kearns, D.; Liu, H.; Consoli, C. Technology readiness and costs of CCS. *Technology* **2021**, *1*, 22–23.
11. Mohammed, I.Y.; Samah, M.; Sabina, G.; Mohamed, A. Comparison of Selexol™ and Rectisol® Technologies in an Integrated Gasification Combined Cycle (IGCC) Plant for Clean Energy Production. *Int. J. Eng. Res.* **2014**, *3*, 742–744. [CrossRef]
12. Bui, M.; Adijman, C.; Bardow, A.; Anthony, E.; Boston, A.; Brown, S.; Fennell, P.; Fuss, S.; Galindo, A.; Hackett, L.A. Carbon capture and storage (CCS): The way forward. *Energy Environ. Sci.* **2018**, *11*, 1064.
13. E.ON UK. Kingsnorth Carbon Dioxide Capture and Storage Demonstration Project—CO₂ Compression and Pumping Philosophy. *E.ON SE* **2011**, *5*, 2–7.
14. Czaplicki, A.; Sobolewski, A. CO₂ emission—Civilization’s progress or investment development inhibiting factor. *Chemik* **2013**, *67*, 387–398.
15. Ahmad, M.; Gersen, S. Water Solubility in CO₂ Mixtures: Experimental and Modelling Investigation. *Energy Procedia* **2014**, *63*, 2402–2411. [CrossRef]
16. Stewart, M.; Arnold, K. *Gas Dehydration Field Manual*; Gulf Professional Publishing: Houston, TX, USA, 2011; pp. 16–24.
17. Allam, R.; Martin, S.; Forrest, B.; Fetvedt, J.; Lu, X.; Freed, D.; Brown, G.W.; Sasaki, T.; Itoh, M.; Manning, J. Demonstration of the Allam Cycle: An Update on the Development Status of a High Efficiency Supercritical Carbon Dioxide Power Process Employing Full Carbon Capture. *Energy Procedia* **2017**, *114*, 5948–5966. [CrossRef]
18. Walspurger, S.; Dijk, H. *EDGAR CO₂ Purity: Type of Quantities of Impurities Related to CO₂ Point Source and Capture Technology*; A Literature Study; Energy Research Centre of the Netherlands: Petten, The Netherlands, 2012; pp. 22–31.
19. Wetenhall, B.; Race, J.M.; Downie, M.J. The effect of CO₂ purity on the development of pipeline networks for carbon capture and storage schemes. *Int. J. Greenh. Gas Control* **2014**, *30*, 197–211. [CrossRef]
20. Grynia, E.; Carroll, J. Niepożądana woda, czyli przegląd procesów osuszania gazu ziemnego. *Szejk* **2013**, *109*, 18–26.
21. Pokrzywniak, C. Analysis of technical solutions and efficiency of glycol-based processes of natural gas drying. *Wiertnictwo Nafta Gaz* **2007**, *24*, 381–389.
22. Nagy, S.; Barczyński, A.; Blicharski, J.; Duliński, W.; Łaciak, M.; Marszałek, J.; Ropa, C.E.; Rybicki, C.; Smulski, R.; Ślizowski, J. *Vademecum Gazownika Tom I. Podstawy Gazownictwa Ziarnego: Pozyskiwanie, Przygotowanie do Transportu, Magazynowanie*; Scientific and Technical Association of Engineers and Technicians of the Oil and Gas Industry: Kraków, Poland, 2014.

23. Øi, L.E.; Fazlagic, M. Glycol dehydration of captured carbon dioxide using Aspen Hysys simulation. In Proceedings of the 55th Conference on Simulation and Modelling (SIMS 55), Modelling, Simulation and Optimization, Linköping University Electronic Press, Aalborg, Denmark, 21–22 October 2014; Volume 108, pp. 167–174.
24. Witkowski, A.; Rusin, A.; Majkut, M.; Rulik, S.; Stolecka, K. *Advances in Carbon Dioxide Compression and Pipeline Transportation Processes*; Springer: Berlin/Heidelberg, Germany, 2015; Volume 3, pp. 13–35.
25. Witkowski, A.; Majkut, M. The impact of CO₂ compression systems on the compressor power required for a pulverized coal-fired power plant in post-combustion carbon dioxide sequestration. *Arch. Mech. Eng.* **2012**, *59*, 2–13. [[CrossRef](#)]
26. Panowski, M.; Zarzycki, R. Analysis of pre-treatment of carbon dioxide separated from flue gas for transportation and storage. *Polityka Energetyczna* **2013**, *16*, 247–253.
27. Eldemerdash, U.; Kamarudin, K. Assessment of new and improved solvent for pre-elimination of BTEX emissions in glycol dehydration processes. *Chem. Eng. Res. Des.* **2016**, *115*, 214–220. [[CrossRef](#)]
28. Neagu, M.; Cursaru, D.L. Technical and economic evaluations of the triethylene glycol regeneration processes in natural gas dehydration plants. *J. Nat. Gas Sci. Eng.* **2017**, *37*, 327–340. [[CrossRef](#)]
29. Sakheta, A.; Zahid, U. Process simulation of dehydration unit for the comparative analysis of natural gas processing and carbon capture application. *Chem. Eng. Res. Des.* **2018**, *137*, 75–88. [[CrossRef](#)]
30. Włodek, T. Selected aspects of carbon dioxide pipeline transportation. *AGH Drill. Oil Gas* **2012**, *29*, 325–335.
31. Parfomak, P.W.; Folger, P. *Carbon Dioxide Pipelines for Carbon Sequestration: Emerging Policy Issues*; CRS Report for Congress; Library of Congress, Congressional Research Service: Washington, DC, USA, 2008.
32. Zhang, Z.; Wang, G.X.; Massarotto, P.; Rudolph, V. Optimization of pipeline transport for CO₂ sequestration. *Energy Convers. Manag.* **2006**, *47*, 702–715. [[CrossRef](#)]
33. McCoy, S.; Rubin, E. An engineering-economic model of pipeline transport of CO₂ with application to carbon capture and storage. *Int. J. Greenh. Gas Control* **2008**, *2*, 219–229. [[CrossRef](#)]
34. Span, R.; Wagner, W. A new equation of state for carbon dioxide covering the fluid region from the triple-point temperature to 1100K at pressures up to 800 MPa. *J. Phys. Chem. Ref. Data* **1996**, *25*, 1509–1596. [[CrossRef](#)]
35. Han, C.; Zahid, U.; An, J.; Kim, K.; Kim, C. CO₂ transport: Design considerations and project outlook. *Curr. Opin. Chem. Eng.* **2015**, *10*, 42–48. [[CrossRef](#)]
36. Nagy, S.; Olajosy, A. Transport rurociągowy dwutlenku węgla oraz układu azot—Dwutlenek węgla. *Rynek Energii* **2010**, *4*, 63–67.
37. Kuczyński, S.; Hendel, J. Application of Monte Carlo simulations for economic efficiency evaluation of carbon dioxide enhanced oil recovery projects. In Proceedings of the 14th International Multidisciplinary Scientific GeoConference SGEM, Albena, Bulgaria, 17–26 June 2014; pp. 663–670.
38. Kuczyński, S.; Hendel, J.; Sikora, A. Economic evaluation of CO₂ enhanced oil recovery and sequestration on small offshore field. In Proceedings of the SGEM 2018 Vienna, Section Oil and Gas Exploration, Vienna, Austria, 3–6 December 2018.
39. Włodek, T.; Kuczyński, S.; Hendel, J. Technical and economic issues of offshore pipeline carbon dioxide transportation. *AGH Drill. Oil Gas* **2014**, *31*, 341–354. [[CrossRef](#)]
40. Abbas, Z.; Mezher, T.; Abu-Zahra, M. Evaluation of CO₂ purification requirements and the selection of processes for impurities deep removal from the CO₂ product stream. *Energy Procedia* **2013**, *37*, 2389–2396. [[CrossRef](#)]
41. Alstom, U.K. *European Best Practice Guidelines for Assessment of CO₂ Capture Technologies*; SINTEF: Trondheim, Norway, 2011.
42. Climate Action-European Commission. *Implementation of Directive 2009/31/EC on the Geological Storage of Carbon Dioxide. Guidance Document 1: CO₂ Storage Life Cycle Risk Management Framework*; Climate Action-European Commission: Luxembourg, 2011.
43. De Visser, E.; Hendriks, C.; Barrio, M.; Mølnvik, M.J.; de Koeijer, G.; Liljemark, S.; Le Gallo, Y. Dynamis CO₂ quality recommendations. *Int. J. Greenh. Gas Control* **2008**, *2*, 478–484. [[CrossRef](#)]
44. Basava-Reddi, L.; Wildgust, N.; Ryan, D. Effects of Impurities on Geological Storage of Carbon Dioxide. In Proceedings of the 1st EAGE Sustainable Earth Sciences (SES) Conference and Exhibition, Valencia, Spain, 8–11 November 2011; European Association of Geoscientists & Engineers: Bunnik, The Netherlands, 2011; p. cp-268.
45. Lako, P.; Van Der Welle, A.J.; Harmelink, M.; Van Der Kuip, M.D.C.; Haan-Kamminga, A.; Blank, F.; Nepveu, M. Issues concerning the implementation of the CCS Directive in the Netherlands. *Energy Procedia* **2011**, *4*, 5479–5486. [[CrossRef](#)]
46. Dooley, J.J.; Dahowski, R.T.; Davidson, C.L.; Wise, M.A.; Gupta, N.; Kim, S.H.; Malone, E.L. *Carbon Dioxide Capture and Geologic Storage: A Core Element of a Global Energy Technology Strategy to Address Climate Change*; GTSP, Pacific Northwest National Laboratory: Richland, WA, USA, 2006; Volume 1, pp. 15–16.
47. Raza, A.; Rezaee, R.; Bing, C.H.; Gholami, R.; Nagarajan, R.; Hamid, M.A. CO₂ storage in heterogeneous aquifer: A study on the effect of injection rate and CaCO₃ concentration. *Mater. Sci. Eng.* **2016**, *121*, 2–3.
48. Volpi, V.; Forlin, E.; Baroni, A.; Estublier, A.; Donda, F.; Civile, D.; Caffau, M.; Kuczyński, S.; Vincké; Delprat-Jannaud, F. Evaluation and Characterization of a Potential CO₂ Storage Site in the South Adriatic Offshore. *Oil Gas Sci. Technol.* **2015**, *70*, 695–712. [[CrossRef](#)]
49. Państwowy Instytut Geologiczny—Zestawienie Projektów Demonstracyjnych i Komercyjnych CCS. Available online: https://skladowanie.pgi.gov.pl/twiki/pub/KAPS/WebHome/ccsww1_2019.xls (accessed on 2 January 2023).
50. Global CCS Institute. *Global Status of CCS 2020*; Global CCS Institute: Melbourne, Australia, 2020.

51. Regulation the Minister of Economy of 26 April 2013 Concerning Technical Conditions to Be Met by Gas Networks and Their Location (Dz.U.2013.640) (PL). Available online: <https://isap.sejm.gov.pl/isap.nsf/download.xsp/WDU20130000640/O/D20130640.pdf> (accessed on 2 September 2021).
52. Rubin, E.; De Coninck, H. *IPCC Special Report on Carbon Dioxide Capture and Storage*; Cambridge University Press: Cambridge, UK, 2005; pp. 117–171.
53. Cole, I.S.; Corrigan, P.; Sim, S.; Birbilis, N. Corrosion of pipelines used for CO₂ transport in CCS: Is it a real problem? *Int. J. Greenh. Gas Control* **2011**, *5*, 749–756. [[CrossRef](#)]
54. PM International Suppliers—API 5L X Grades. Available online: <https://www.api5lx.com/api5lx-grades/> (accessed on 2 September 2021).
55. Peng, D.; Robinson, D.B. A New Two-Constant Equation of State. *Ind. Eng. Chem. Fundam.* **1976**, *55*, 59–64. [[CrossRef](#)]
56. Rulik, S.; Witkowski, A. Selecting the configuration of inter-stage coolers for a CO₂ compressor. *J. Power Technol.* **2015**, *95*, 4–9.
57. Petroskills John, M. Campbell—Transportation of CO₂ in Dense Phase. Available online: <http://www.jmcampbell.com/tip-of-the-month/2012/01/transportation-of-co2-in-dense-phase/> (accessed on 2 January 2023).

Disclaimer/Publisher’s Note: The statements, opinions and data contained in all publications are solely those of the individual author(s) and contributor(s) and not of MDPI and/or the editor(s). MDPI and/or the editor(s) disclaim responsibility for any injury to people or property resulting from any ideas, methods, instructions or products referred to in the content.